An Implicit Loop Method for Kinematic Calibration and Its Application to Closed-Chain Mechanisms

Charles W. Wampler, *Member, IEEE*, John M. Hollerbach, *Member, IEEE*, and Tatsuo Arai, *Member, IEEE*

Abstract— A unified formulation for the calibration of both serial-link robots and robotic mechanisms having kinematic closed-loops is presented and applied experimentally to two 6-degree-of-freedom devices: the RSI 6-DOF Hand Controller and the MEL "Modified Stewart Platform." The unification is based on an equivalence between end-effector measurements and constraints imposed by the closure of kinematic loops. Errors are allocated to the joints such that the loop equations are satisfied exactly, which eliminates the issue of equation scaling and simplifies the treatment of multi-loop mechanisms. For the experiments reported here, no external measuring devices are used; instead we rely on measurements of displacements in some of the passive joints of the devices. Using *a priori* estimates of the statistics of the measurement errors and the parameter errors, the method estimates the parameters and their accuracy, and tests for unmodeled factors.

I. INTRODUCTION

THE implicit loop method for kinematic calibration is founded on an equivalence between displacement measurements and kinematic closed-loops. For example, docking a robot's end-effector into a mechanical fixture that determines its position and orientation is equivalent to a measurement of the location of the end-effector by other means, such as theodolites or laser interferometry. Clearances between mating surfaces of the fixture and end-effector yield uncertainties that correspond to measurement error. If we consider the end-effector to have a (typically) 6 degree-of-freedom "joint" with respect to ground, measurements of the end-effector location may be regarded as joint measurements. With this convention, the kinematic model of any mechanism—open-chain or closed-chain—becomes a statement that the displacements around a closed loop must sum to zero.

Whenever the total number of joint measurements (including the end-effector "joint") exceeds the number of degrees of freedom of motion, the kinematic equations predict dependencies between the measured quantities. A set of measurements

taken at various poses of the mechanism is not likely to satisfy these equations exactly; such discrepancies must be explained by some combination of measurement error and error in the parameters of the kinematic model (including also the sensor parameters, such as gains or offsets). We look for the most likely combination of such errors that satisfy the kinematic equations exactly. The answer depends upon statistical models of the distribution of both measurement errors and errors in the parameters of the mechanism. The result will be our best estimate of the true values of the parameters in light of the given measurements.

The term "implicit loop method" emphasizes that the errors enter the kinematic loop equations implicitly, rather than being explicit outputs of a conventional input-output formulation. By removing the requirement to express errors explicitly, the formulation allows the analyst to concentrate on correctly attributing all sources of error. For example, a typical formulation for a serial-link robot finds kinematic parameters that minimize the difference between the measured end-effector location and the prediction of the model. But the differences may in fact be due to errors in the joint angle measurements ("input noise," in statistical parlance). By not acknowledging this potentially significant source of error, the parameter estimates may be biased. In contrast, the implicit loop method puts joint and end-effector measurements on equal footing, with weights assigned according to the accuracy of each. A more complete picture of the implicit loop method's place in the context of current practice is available in [1].

The method is illustrated in experiments on two in-parallel mechanisms. Overviews of the robot calibration literature [2]–[4] reveal that until recently almost all investigations considered only the serial-link case. Calibration of robots with closed loops was considered in [5] and 6-in-parallel RRPRRR platforms were studied in [6]. Bennett and Hollerbach [7] considered serial-link arms that form a closed loop by interacting with their environment. This work is similar to ours in that the calibration is performed using only measurements of the robot's internal joint motions, with no external devices required. These simulation studies have been followed by experiments by several researchers [8], [9]. This paper presents a re-analysis of the Hollerbach and Lokhurst experiments and also describes a new experiment using the MEL Modified Stewart Platform.

We begin by reviewing our method of analysis, previously outlined in [10]. We use a statistical maximum-likelihood criterion, formulated to handle the kind of implicit measurement equations that arise in closed-chain calibration experiments.

The usefulness of this approach is illustrated in its application to the two calibration experiments.

II. METHOD OF ANALYSIS

The minimization criterion should strike a balance between the errors attributed to the various measurements and the corrections applied to the parameters. These should be commensurate with our *a priori* notions of the accuracy of the sensors and the accuracy of the techniques used to build the mechanical device. We adopt a statistical approach, based on the maximum-likelihood principle. At heart, this is simply a least-squares fit, where the weighting factors have been chosen according to the variances of the sources of uncertainty in the model: measurement error, manufacturing tolerances, and joint looseness. Besides providing a rationale for picking weighting factors, the statistical approach provides two other important results, namely, estimates of the accuracy of the fitted parameters, and a measure of the consistency of the data with the model. Without checks of this kind, we would not know whether the calibration was providing significantly improved model parameters and would not have any indication whether or not some significant factor had been left out of the model. Such checks can be generated through extensive Monte Carlo simulation, but a statistical approach can derive these results quite straightforwardly from a linear analysis of the fitting process.

In the context of serial-link robots with an explicit model of end-effector measurements, some previous formulations have allowed for joint angle measurement noise [11], [12]. Related formulations that allow input noise have appeared in the statistical literature under various appellations: "total least squares" [13, Section 10.3], "error-in-variables models" [14], and "orthogonal distance regression" [15]. Especially for closed-loop linkages, we find it convenient to reformulate with all variables appearing implicitly. An explicit formulation can be considered a special case. The additional inclusion of *a priori* statistics on the parameter corrections has appeared in [2], [11].

A. Implicit Loop Formulation

Let us assume that we can write the kinematic model of the robot as

$$f(x, p) = 0, \qquad f: R^k \times R^n \to R^m \qquad (1)$$

where $x \in R^k$ is a vector of motion variables and $p \in R^n$ is the vector of parameters to be calibrated. The vector x may include joint and end-effector displacements that we measure, as well as backlashes or other small unknown displacements. We require $k \geq m$ and rank $(\partial f / \partial x) = m$ to guarantee that the loop can always be closed. We also assume that unmeasured joint motions have been eliminated from the kinematic equations.[1] Parameters include the geometry of the links (such as Denavit–Hartenberg parameters) and parameters

[1] If some unmeasured joint displacements cannot be eliminated, they can be solved numerically as part of the iterative solution. However, the convergence of the method will then be dependent on having sufficiently good initial guesses for these joints.

of the sensors, such as gains or offsets. Each of the m equations in f derives from the sum of displacements around a closed loop in the mechanism. This is meant to include "loops" where one leg of the loop is the measured displacement of the end-effector. In this manner, open-loop chains with measurement of one or more components of the end-effector displacement are treated by the same formulation.

We will move the robot to various poses, obtaining for each pose a measurement of x. Let x_i be the value of x at the ith pose, which we measure as $\overline{x}_i$ with measurement error $\hat{x}_i$, so $x_i = \overline{x}_i + \hat{x}_i$. (An unmeasured noise factor, which we might use to model a backlash, for example, can be included by setting $\overline{x}$ to the expected mean.) Throughout all of the sample poses, the parameters should be constant, but our initial estimates $\overline{p}$ of the parameters may be in error by $\hat{p}$. That is, $p = \overline{p} + \hat{p}$. For example, $\overline{p}$ might be the blueprint value of a link length and $\hat{p}$ would then be the error incurred in manufacturing the part. Accordingly, we write the loop equations at the ith sample as

$$f(x_i, p) = f(\overline{x}_i + \hat{x}_i, \overline{p} + \hat{p}) = 0, \qquad i = 1, \cdots, N \quad (2)$$

where N is the number of sample positions. Notice that in this implicit model we do not distinguish between "inputs" and "outputs," but rather we have only "measurements," each with an associated variance.

The objective of the calibration is to find a value for $\hat{p}$ that will improve the accuracy of our kinematic model. Of all possible combinations of parameter error $\hat{p}$ and measurement noises $\hat{x}_i$ that agree with our kinematic model, (2), we wish to find the most likely combination. Recall that a vector η of Gaussian noise having zero mean and covariance Σ has a probability density function proportional to $e^{-\eta^T \Sigma^{-1} \eta / 2}$ [16, Section 10.7], and hence maximizing the probability is the same as minimizing $\eta^T \Sigma^{-1} \eta$. Suppose the errors $\hat{x}_i$ and $\hat{p}$ are independent, Gaussian noises with means equal to zero and with covariances as follows: $\text{Var}(\hat{x}_i) = E(\hat{x}_i \hat{x}_i^T) = \Sigma_x$, $\text{Var}(\hat{p}) = \Sigma_p$. Then the maximum-likelihood estimate is the minimizer of

$$\chi^2 = \sum_{i=1}^{N} \hat{x}_i^T \Sigma_x^{-1} \hat{x}_i + \hat{p}^T \Sigma_p^{-1} \hat{p}, \qquad (3)$$

subject to (2). Note that the assumption of zero mean is easily satisfied because a known bias can be subtracted out, while an unknown one can be included as a parameter. (For simplicity, we have assumed the covariance matrix Σ_{x_i} of the ith measurement error $\hat{x}_i$ is the same for all i; hence we write Σ_x. To allow covariances that vary with the sample, one need only to carry the extra subscript through all of the equations that follow.)

An important feature of this formulation is that we require the kinematic equations to be satisfied exactly, accounting for any discrepancies implicitly via the measurement and parameter errors. This is in contrast to the standard approach wherein the residual error in the equations is minimized. In the standard approach, the best fit depends on the scaling of the various equations, some of which may involve orientation while others concern position. Furthermore, we often can

write several loop equations of which only a subset are linearly independent. The best fit then depends on which subset of equations is used. In [6], this was addressed by considering sums of squared error of all possible loops. In contrast, when the kinematic equations are satisfied exactly, the result is independent of equation scaling and independent of which set of loop equations we choose. The issue of scaling between position and orientation is settled when we specify the covariances Σ_x and Σ_p.

Least-squares estimation has a venerable history, but perhaps a few words concerning its validity in the current context are warranted. It can be shown that, under the assumption of Gaussian distributions and linear model equations, the minimum-variance estimate, the maximum-likelihood estimate and the (Bayesian) conditional-expected-value estimate are all identical [16, Section 12.2]. By the Central Limit Theorem of probability, the distribution of errors will be approximately Gaussian if they are actually the sums of many independent errors (none of which dominate). Moreover, a linearization of the loop equations around each sample position will be reasonably accurate for small enough measurement and parameter errors. Hence, the assumptions of Gaussian noise and linearity are often plausible, and all three estimation principles lead to the same least-squares problem. While one might sometimes be able to verify these assumptions in detail, often one must fall back on the more basic justification that the least-squares approach will usually yield an estimate for which the magnitudes of $\hat{x}_i$ and $\hat{p}$ are not far from the level of error we expect and, moreover, the approach is easy to apply and to analyze. Since the parameters usually include a variety of quantities, such as lengths, angles, sensor gains, and so on, it is important that they be scaled appropriately before combining them into a least-squares criterion. The statistical approach of using variances is a logical way to arrive at such a scaling.

The most common phenomenon which will cause least-squares estimation to degenerate is the presence of "outliers" in the data. A single measurement far outside the expected deviation can badly skew the results. If outliers are a problem, one needs to model the errors with a distribution that is broader than Gaussian. Some practical suggestions are given in [17, Section 14.6]. Another contradiction of the Gaussian assumption may arise if backlash is a dominant phenomenon. Backlash errors tend to be bimodal, that is, the backlash will tend to be at one of two extremes, depending on the last direction of travel. A model that accounts for the last direction of travel may restore validity of the Gaussian assumption.

The inclusion of the parameter errors $\hat{p}$ in the least-squares criterion expresses our belief, prior to performing the calibration, that the actual parameters of the device will be close to the "blueprint" values. Ideally, the variance Σ_p would come from an appraisal of the tolerances that enter into the manufacture and assembly of the robot. The calibration will adjust the parameters away from the blueprint values only to the extent that the measurements produce convincing evidence. Previous researchers have sometimes omitted this factor (see survey in [2]). Omission of this factor is consistent with the assumption that the measurements are very accurate compared to the parameter errors, hence Σ_p^{-1} is small relative

to Σ_x^{-1} and can be ignored. However, there often exist combinations of parameter errors that are weakly measured, so that the associated measurement errors are effectively magnified. Accordingly, it is wise to include Σ_p as a safeguard. In the analyses reported below, we find that Σ_p^{-1} is not negligible.

B. Solution

One could formulate the minimization of (3) subject to (2) as a Lagrangian:

$$\mathcal{L} = \chi^2 + \sum_{i=1}^{N} \lambda_i^T f(\overline{x}_i + \hat{x}_i, \overline{p} + \hat{p}), \tag{4}$$

where the λ_i are Lagrange multipliers. The extremal equations for the minimization are obtained from the first derivatives of (4). If these were solved by Newton's method, quadratic convergence would be expected, but the second derivatives of f would be needed. The following iterative solution procedure neglects the second derivatives of f. This simplifies the method at the expense of a slower (linear) rate of convergence. It can be shown that the equilibrium conditions for the iterations are the same as the extremal equations for the Lagrangian.

Appendix I contains derivations for the following steps. First, introduce normalized error variables $y_i \in R^k$ and $q \in R^n$, having unit covariances $\text{Var}(y_i) = I$ and $\text{Var}(q) = I$. Then set

$$\hat{x}_i = \Sigma_x^{1/2} y_i, \qquad \hat{p} = \Sigma_p^{1/2} q, \tag{5}$$

where the superscript $1/2$ means the symmetric square root. (In the common case that the individual elements of $\hat{x}_i$ and $\hat{p}$ are all independent, $\Sigma_x^{1/2}$ and $\Sigma_p^{1/2}$ are diagonal matrices, whose elements are standard deviations.) Substitution of (5) into (3) gives

$$\chi^2 = \sum_{i=1}^{N} y_i^T y_i + q^T q. \tag{6}$$

Note that the new variables y_i and q are dimensionless.

Begin the iteration with an initial guess of $y_i = 0$ and $q = 0$. At each step, find corrections Δy_i and Δq to minimize

$$\sum_{i=1}^{N} (y_i + \Delta y_i)^T (y_i + \Delta y_i) + (q + \Delta q)^T (q + \Delta q), \tag{7}$$

subject to the linearized constraints

$$J_{yi}\Delta y_i + J_{qi}\Delta q = -f(\overline{x}_i + \Sigma_x^{1/2} y_i, \overline{p} + \Sigma_p^{1/2} q),$$
$$i = 1, \cdots, N \tag{8}$$

where J_{yi} and J_{qi} are matrices of partial derivatives obtained using the chain rule:

$$J_{yi} = \frac{\partial f}{\partial x}(\overline{x}_i + \Sigma_x^{1/2} y_i, \overline{p} + \Sigma_p^{1/2} q) \Sigma_x^{1/2}$$
$$J_{qi} = \frac{\partial f}{\partial p}\left(\overline{x}_i + \Sigma_x^{1/2} y_i, \overline{p} + \Sigma_p^{1/2} q\right) \Sigma_p^{1/2}. \tag{9}$$

Instead of carrying along a full set of variables $\{\Delta y_i (i = 1 \cdots, N), \Delta q\}$, one may perform an orthogonal decomposition on the ith set of constraint equations to eliminate Δy_i as follows. First, compute a QR-decomposition[2] of the Jacobian matrices:

$$Q_i R_i = J_{yi}^T. \qquad (10)$$

Then, set

$$D_i = R_i^{-T} J_{qi}$$
$$E_i = Q_i^T y_i - R_i^{-T} f(\overline{x}_i + \Sigma_x^{1/2} y_i, \overline{p} + \Sigma_p^{1/2} q) \qquad (11)$$

whereupon the step in q is the least-squares solution to the overconstrained linear system

$$\begin{pmatrix} D_1 \\ \vdots \\ D_N \\ I \end{pmatrix} \Delta q = \begin{pmatrix} E_1 \\ \vdots \\ E_N \\ -q \end{pmatrix}, \qquad (12)$$

and the updated error estimates are

$$y_i + \Delta y_i = Q_i (E_i - D_i \Delta q). \qquad (13)$$

Replacing y_i with $y_i + \Delta y_i$ and q with $q + \Delta q$, (9)–(13) can be iterated until convergence.

C. Error Analysis

In what follows, it is convenient to denote the "fitting matrix" D and the "augmented fitting matrix" $\hat{D}$ as follows:

$$D = (D_1^T \cdots D_N^T)^T,$$
$$\hat{D} = (D^T \quad I)^T. \qquad (14)$$

Neglecting the effects of higher-order terms in f and assuming Gaussian distributions, the covariance of the error between the estimated q and the true value q^* is (see Appendix II)

$$\Sigma_q = \text{Var}(q - q^*) = (\hat{D}^T \hat{D})^{-1}. \qquad (15)$$

Reversing the normalization, the accuracy of the estimated parameters p compared to their actual values p^* is zero mean with covariance

$$\Sigma_p' = \text{Var}(p - p^*) = \Sigma_p^{1/2} \Sigma_q \Sigma_p^{1/2}. \qquad (16)$$

Since $D_i^T D_i$ is necessarily positive, semi-definite, one may see that every measurement reduces the covariance of the estimates, although the actual decrease may be small. In particular, if a measurement has a large covariance Σ_x, it will give a small D_i and the effect on the estimate will also be small.

It is very common that some components of the estimate are much less accurate than others. Let the singular value decomposition of the fitting matrix be $D = USV^T$, that is, U and V are orthogonal matrices and $S \in R^{(Nm) \times n}$ has entries $S_{ij} = 0 \ (i \neq j)$, $S_{ii} = s_i$, $s_1 \geq s_2 \geq \cdots \geq s_n \geq 0$. The scalars $s_1, \cdots, s_n$ are called the singular values. The columns

---

[2] Any $m \times n$ matrix A, $m \geq n$, can be written as $A = QR$, where the columns of Q are orthonormal and R is an $n \times n$ upper triangular matrix.

---

of V associated with the small singular values are the linear combinations of the normalized q parameters that are not well measured. Noting that $\hat{D}^T \hat{D} = V(I + S^T S)V^T$, we write

$$\Sigma_q = V[\text{diag}(\cdots, 1/(s_i^2 + 1), \cdots)]V^T, \qquad (17)$$

which shows that the columns of V are independent error directions with the ith column having standard deviation $1/\sqrt{s_i^2 + 1}$. Since the initial standard deviation in each direction is 1, we may say that $1/\sqrt{s_i^2 + 1}$ is the fraction of the initial error remaining after calibration. When the measurement is noisy compared to the initial error, s_i will be small ($s_i \ll 1$), the standard deviation of the associated error direction will remain at its original value of 1, and the estimate will be unchanged from the "blueprint" values. When the experimental data is strong, we will obtain $s_i \gg 1$ and a standard deviation of approximately $1/s_i$.

D. Goodness of Fit

It is good to check if the results of the estimation agree with statistical assumptions of the model. One such measure of goodness-of-fit is to compute the value of χ^2 from (6) for the converged values of (y_i, q). If the Gaussian assumptions are valid, χ^2 has an expected value of Nm with standard deviation $\sigma = \sqrt{2Nm}$. The exact distribution of χ^2 can be computed in terms of gamma functions or found in a table of statistical functions, but for large enough Nm, say $Nm > 30$, it is well-approximated by a Gaussian distribution. In that case, χ^2 should fall within $\pm 3\sigma$ of its expected value 99.7% of the time, so a result outside of this interval casts serious doubt that the experiment is consistent with the model.

If the χ^2 is unexpectedly high, the most likely causes are either: the variances of the measurement errors or the *a priori* parameter errors have been set too small, or some significant factor has been neglected in the model. A third possibility is non-Gaussian error distributions, especially outliers. If an explanatory factor cannot be found, one can always bring the χ^2 into range by raising the initial variances Σ_x and Σ_p. This will have the effect of increasing Σ_p', the estimate of the variance in the fitted parameters. However, if the initial variances must be raised implausibly high, the results are not trustworthy: a better model is needed.

We can also double check the model by re-calibrating several times and comparing the results. Since two experiments will never return exactly the same results, the comparison should take into account the statistics of the process. Two calibration experiments on the same device are not independent, because although they presumably have independent measurement errors, they have the same underlying parameter errors. The relevant formulas are derived in Appendix III. Let p_1 and p_2 be parameters estimated from two different experiments, and suppose the covariance for $p_1 - p_2$ is a full rank matrix $\Sigma_{1,2}$. Then $(p_1 - p_2)^T \Sigma_{1,2}^{-1}(p_1 - p_2)$ is a chi-square with n degrees of freedom.

E. Relation to Kalman Filters

It is interesting to note the relation of our estimator to common forms of the Kalman filter. In filter form, the samples

are processed sequentially, producing a new estimate after every sample. This corresponds to adding one more block to (12) after each sample. It is standard to use recursive least-squares so that only the most recent block is in storage at each sample update, which can become a critical consideration if the number of samples becomes large enough. According to the classification of [18], if all the blocks are linearized around the initial guess, we have the *linearized Kalman filter*. If each block is linearized about the current estimate (based on all the previous samples), we have the *extended Kalman filter*. In either case, it is usual to take only one step of (12) at each sample. We have advocated iterating so that the nonlinear effects of the kinematics are more fully taken into account.

F. Serial-Link Robots

The most common formulation for the calibration of serial-link robots is to find parameter values that minimize (in a least-squares sense) the difference between measured end-effector locations and the locations predicted by a forward kinematic model. Here, "location" means 6 DOF position and orientation or any subset of the 6 components thereof. This usual approach ignores errors in the joint angle measurements and does not use *a priori* knowledge of the parameter values to dampen weakly measured components of the parameter errors. Depending on the actual circumstances of the experiment, these omissions may be justified and some simplification garnered as a result. In the absence of a statistical formulation, care should be taken to properly scale position and orientation errors. In our formulation, the covariance matrix for measurement errors provides this scaling.

The simplifying assumptions of the standard approach are not always valid. Even when an actuator rotation is measured with a highly accurate optical encoder, there is often a gear train between the encoder and the actual joint, which may introduce a significant error to the implied joint angle measurement. Furthermore, one may justifiably neglect prior knowledge of the statistics of the parameter errors only if the experiment is sufficiently well-conditioned and the end-effector measurements sufficiently accurate so that all the parameters are determined to within an error that is negligible compared to that prior knowledge. Of course, it is highly desirable for this to be so, but it is not always the case. The more general formulation presented here will allow us to quantify these assumptions and to proceed when these assumptions do not hold. When the assumptions do hold, we will get the same results.

For the case of serial-link arms, similar formulations to ours have appeared previously. Zak *et al.* [12] allow for joint-angle errors and Renders *et al.* [11] additionally include a covariance on parameter errors. The latter is also mentioned in [2]. All of these linearize the kinematic equations, and will produce the same result as the first iteration of our method when equivalent assumptions regarding covariances are applied.

III. CALIBRATION OF THE RSI 6DOF HAND CONTROLLER

Hollerbach and Lokhurst [8] have reported on experiments in calibrating the RSI Hand Controller, which is a six-degree-
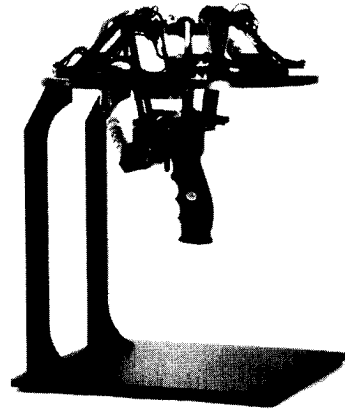

Fig. 1. RSI 6-DOF hand controller.

of-freedom joystick that measures the motion of a handle in a workspace of ±3 in (75 mm) translation and ±30° rotation in any direction (see Fig. 1). The handle is mounted to an endplate that is connected to a stationary base by 3 indentical 6R serial linkages. Each linkage is a kind of elbow arm with a spherical wrist connecting to the endplate. Potentiometers measure the two shoulder joint angles and the elbow joint angle, from which the positions of the wrist centers, and therefore the position and orientation of the handle, can be inferred. Since there are a total of 9 angle measurements (3 per elbow arm) and the overall mechanism has only 6 degrees of freedom, the excess 3 measurements can be used to calibrate the internal dimensions of the device. The redundant information in the measurements is associated with the fact that the inferred positions of the wrist points should conform to known fixed distances between them, as established by their rigid mounting to the endplate.

This section describes a re-analysis of the experimental results of [8], to which we refer the reader for the details of the kinematics of the device and the experimental procedure. Two main experiments were conducted. In the first, the endplate was accurately located (position and orientation) in 12 poses using a special fixture. Joint angle readings were recorded for each pose. Since the poses are known accurately, this experiment provides an excess of 9 measurements per pose that can be used for calibration. In the second experiment, the handle was manually placed near a pre-planned set of 12 poses. Since the true location of the handle is unknown in this case, there are only 3 extra measurements per pose for use in calibration.

We will use the statistical methods of the previous section to do the following:

1) Replicate Hollerbach and Lokhurst's results while additionally providing estimates of the accuracy of the calibration.
2) Recompute a calibration using a different model of the measurement error. This is to illustrate the flexibility of the formulation.
3) Statistically compare the results of the two experiments (fixtured versus free).

In all cases, we assume that the machining and assembly of the mechanism is precise enough that we need only to calibrate

the joint angle sensors. Let θ be a 9×1 column of joint angles, related to the column of potentiometer readings α by gains κ and offsets θ^{off} as

$$\theta_i = \kappa_i(\alpha_i - 2048) + \theta_i^{\text{off}}, \qquad i = 1, \cdots, 9, \qquad (18)$$

where 2048 is the A/D reading at zero volts. During assembly, the potentiometers were set to read 0.00 V at the rest position, where the nominal offsets are $(0.42, -1.97, 0.02)$ rad for each arm. All potentiometers have $340°$ range and readings are recorded using a 12-bit A/D converter, giving a nominal gain of $-0.001\,45$ rad/bit. The objective of the calibration will be to estimate κ and θ^{off} by computing corrections $\hat{\kappa}$ and $\hat{\theta}^{\text{off}}$. We assume standard deviations on these parameter errors of $0.000\,05$ rad/bit and 0.05 rad, respectively. These were rough estimates chosen such that a $\pm 3\sigma$ gain error would be $\pm 10\%$ of the nominal gain and $\pm 3\sigma$ in the offset angles would comfortably bracket the manual error in setting the zero points of the potentiometers.

The kinematics of the device can be summarized as follows. Let $r_i(\theta)$ be the position of the ith wrist point $(i = 1, 2, 3)$ in base coordinates, computed from the joint angles using the forward kinematics of the ith arm. In the experiments where the calibration fixture determines the endplate position and orientation, denoted P, R, we may write

$$r_i(\theta) - (P + Rw_i) = 0, \qquad i = 1, 2, 3, \qquad (19)$$

where w_i is the location of the ith wrist point in the frame of the endplate. Without the fixture, we have only that the wrist points are constrained by the endplate to lie on an equilateral triangle of side d, so

$$[r_i(\theta) - r_j(\theta)]^2 - d^2 = 0,$$
$$(i, j) = \{(1, 2), (2, 3), (3, 1)\}. \qquad (20)$$

Note that in (20), each loop equation involves two arms, and hence the equations are coupled. For simplicity, we could ignore this and calibrate one loop at a time, but for a given set of measurements we will obtain better accuracy by considering all the loops simultaneously. To see this, note that when two loops are considered independently on the same set of measurements, they predict different parameter and measurement errors for their common arm. This contradiction is resolved when the two loops are considered simultaneously. In (19), the loops are coupled if P and R are ascribed to have measurement error, but are independent if these are considered exact.

A. Model 1: Fixtured Calibration

To establish a baseline set of parameters, let us begin with the more accurate experiment using a mechanical fixture to accurately locate the end-effector. From (19), we have model equations as follows:

$$f_i = \begin{cases} r_1(\theta_i) - (P_i + R_i w_1) \\ r_2(\theta_i) - (P_i + R_i w_2) \\ r_3(\theta_i) - (P_i + R_i w_3) \end{cases} = 0,$$
$$i = 1, \cdots, N. \qquad (21)$$

TABLE I
ESTIMATED PARAMETER CORRECTIONS $\hat{p}$ FOR RSI HAND CONTROLLER

$\hat{p}$	Fixture		No Fixture		
	H&L I	Model 1	H&L II	Model 2	Model 3
(mrad)					
θ_{11}	−52	-53	−42	−34	−39
θ_{12}	−30	−32	−40	−45	−44
θ_{13}	−45	−45	−54	−52	−50
θ_{21}	13	13	20	24	20
θ_{22}	29	27	14	13	20
θ_{23}	27	25	23	22	23
θ_{31}	−43	−44	−43	−36	−39
θ_{32}	−4	−4	−5	−10	−9
θ_{33}	30	29	35	34	32
(μrad/bit)					
κ_{11}	−17	−24	5	13	8
κ_{12}	−46	−57	−97	−62	−70
κ_{13}	48	46	32	34	29
κ_{21}	20	13	5	4	5
κ_{22}	12	4	−3	3	−3
κ_{23}	−23	−10	−20	−14	−21
κ_{31}	−8	−11	−10	−5	−5
κ_{32}	1	−7	−10	8	6
κ_{33}	2	3	8	12	5

Each of these is a vector equation, so we have the equivalent of $m = 9$ scalar equations at each pose i. Hollerbach and Lokhurst formulated this problem by explicitly computing joint angles corresponding to the pose position and orientation (i.e., using the inverse kinematics of the device) and directly comparing these to the measured joint angles. Here, the inverse kinematics are solved implicitly as part of the fitting procedure. Besides not requiring an explicit inverse kinematic calculation, the current formulation allows us to easily include measurement errors on the pose information according to the accuracy of the jig fixture.

In (18) we assume a measurement error on each joint sensor:

$$\alpha_i = \overline{\alpha}_i + \hat{\alpha}_i, \qquad i = 1, \cdots, N. \qquad (22)$$

In addition, we assume additive errors on the 3 components of P_i and on three roll-pitch-yaw Euler angles ψ_i defining $R_i = R(\psi_i)$. We further assume that all of these errors can be approximated as Gaussian distributions. In the notation of Section II, we have measurements $\overline{x}_i = (\overline{\alpha}_i, \overline{p}_i, \overline{\psi}_i)$ with additive error $\hat{x}_i$, both of dimension 15. We also have 18 nominal parameters $\overline{p} = (\kappa_{\text{nom}}, \theta^{\text{off}}_{\text{nom}})$ for which we will estimate corrections $\hat{p} = (\hat{\kappa}, \hat{\theta}^{\text{off}})$.

With this model, we estimate parameters using the $N = 12$ measurements of Hollerbach and Lokhurst in their "open-loop" experiment. To follow the formulation of Section II, we need a priori estimates of the accuracy of the measurements. Assuming standard deviations of 2.5 bits on $\hat{\alpha}$, 0.01 in on P, and 0.005 rad on R, we obtain a chi-square value $\chi^2 = 109$ matching the expected value $Nm = 108$. (To obtain this close match, we doubled our initial estimates of the measurement error.) The parameter corrections $\hat{p}$ are listed in Table I as "Model 1." The expected error, given as the square-root of the diagonal of the 18×18 covariance matrix Σ'_p from (16), is listed in Table II. Correlations between these errors are given by the off-diagonal entries of Σ'_p, which for brevity we do not list.

TABLE II
FITTING STATISTICS

	Model 1	Model 2	Model 3
actual χ^2	109.1[a]	19.7	19.3
expected χ^2	108	36	36
99% range	73.8–149.7	17.9–61.5	17.9–61.5
standard error[b]			
(mrad)			
$\sigma(\theta_{11})$	2	10	9
$\sigma(\theta_{12})$	3	10	10
$\sigma(\theta_{13})$	1	8	7
$\sigma(\theta_{21})$	3	9	7
$\sigma(\theta_{22})$	2	11	10
$\sigma(\theta_{23})$	2	7	7
$\sigma(\theta_{31})$	2	9	9
$\sigma(\theta_{32})$	2	11	10
$\sigma(\theta_{33})$	1	7	7
(μrad/bit)			
$\sigma(k_{11})$	9	16	15
$\sigma(k_{12})$	7	29	27
$\sigma(k_{13})$	5	16	16
$\sigma(k_{21})$	9	17	16
$\sigma(k_{22})$	6	25	23
$\sigma(k_{23})$	8	15	14
$\sigma(k_{31})$	9	17	18
$\sigma(k_{32})$	7	30	31
$\sigma(k_{33})$	5	15	15
Singular values[c]			
maximum	48.7	44.4	39.8
minimum	4.8	0.7	0.8

[a] Scaled *a posteriori* to match expected value.
[b] Square root of diagonal of covariance Σ'_p.
[c] Singular values of fitting matrix D.

For comparison, we may re-construct the estimate of Hollerbach and Lokhurst by assuming the calibration fixture is exact and placing no weight on our *a priori* knowledge of the parameter values. That is, $\hat{x} = \hat{\alpha}$ and $\Sigma_p \to \infty$. (Numerically the latter was accomplished by setting Σ_p to 10^5 times its former value.) The result is given in Table I as "H&L I." With the same *a priori* variances as above, the chi-square value is 137 compared to an expected value of $Nm - n = 90$, which is rather high. To explain this high value, we must presume either that the measurement errors are even worse (approx. 3 bits), the fixture is not exact (as in Model 1), or some new source of error (e.g., link length errors or backlashes). In any case, the estimates H&L I and Model 1 agree well to the accuracy reported in Table II, with the worst disagreement in k_{12} being 1.6 times the quoted standard error.

For our Model 1, the maximum and minimum singular values of the fitting matrix D are 48.7 and 4.83, respectively, which gives a very mild condition number of 10. As discussed at (17), these singular values imply that the parameter error has been reduced to just 2% of its initial value in the best direction and to 20% of the initial value in the most poorly measured direction. The sizes $|\Delta q|$ of the iterative steps are 2.5, 3.1e-1, 8.2e-2, 4.3e-2, etc., which is a rather slow, linear rate of convergence.

B. Model 2: Wrist Errors

Next we consider measurements taken without the aid of the calibration fixture. A variety of errors (e.g., looseness in

joints, link dimension errors, sensor noise) will prevent strict equality in (20). One approach is to lump these together into a single error term for each equation, giving three equations per sample pose as follows:

$$f_i = \begin{cases} [r_1(\theta_i) - r_2(\theta_i)]^2 - d^2 + \epsilon_{1i} \\ [r_2(\theta_i) - r_3(\theta_i)]^2 - d^2 + \epsilon_{2i} \\ [r_3(\theta_i) - r_1(\theta_i)]^2 - d^2 + \epsilon_{3i} \end{cases} = 0,$$
$$i = 1, \cdots, N. \tag{23}$$

In the experiment, the number of poses was $N = 12$. If the error terms ϵ_{ki} can be approximated as Gaussian distributions, we may apply the formulation of Section II with the following correspondences: $\bar{x}_i = 0$, $\hat{x}_i = (\epsilon_{1i}, \epsilon_{2i}, \epsilon_{3i})$, $\bar{p} = (\kappa_{\text{nom}}, \theta_{\text{nom}}^{\text{off}})$, and $\hat{p} = (\hat{\kappa}, \hat{\theta}^{\text{off}})$. Because of the lumped error model, the Jacobian matrix $\partial f_i / \partial x_i$ is the identity matrix, and (9)–(13) could be simplified to save computer time.

With this model we estimate parameters using the $N = 12$ measurements of Hollerbach and Lokhurst in their "closed-loop" experiment. Lacking a good estimate of the variance of $\hat{x}$, we proceeded by trial-and-error to determine what value would give a consistent chi-square value for the fit. The units of the errors ϵ_{ki} are in^2. Assuming the ϵ_{ki} to be independent with equal variances, we found after a few trials that a standard deviation of 0.1 in^2 gave $\chi^2 = 19.7$. The expected value for χ^2 is $3 \cdot 12 = 36$ with standard deviation $6\sqrt{2} \approx 8.5$, so this is in the right range.

Some rough calculations can check if 0.1 in^2 is plausible. If backlash at each wrist joint contributes a standard deviation of σ to the distance d, the resulting standard deviation in d^2 is $2\sqrt{2}d\sigma$. Accordingly, since $d \approx 2.6$ in, a backlash of $\sigma = 0.014$ in is sufficient to account for the 0.1 in^2 variance in d^2. Alternatively, we can reflect the wrist errors back to the joint angles. Roughly speaking, the wrist point is about 4 in from the joint axes (in the home position), which works out to angular errors in the range 0.002–0.003 rad. That is about 2 bits at the A/D converters, which is not far from the 2.5 bits estimated in Model 1. A more direct and detailed analysis of joint sensor errors is presented in the next section.

As before, we can reconstruct the results of Hollerbach and Lokhurst by setting $\Sigma_p \to \infty$. These results are listed in Table I under the heading "H&L II" along side the Model 2 results. These calibrations are computed from the same set of measurements, but Hollerbach and Lokhurst did not include any weight on the nominal values of the parameters. The two sets of parameters are substantially the same. The minor differences between the two results is attributable to the more poorly measured combinations of parameters, for which the experimental uncertainty is nearly as big or bigger than the initial uncertainty in the parameters.

Table II summarizes the uncertainty in the results. Since the covariance matrix for the parameter estimation error is 18×18, we report only the square root of its diagonal elements. Also, the maximum and minimum singular values of the fitting matrix D are listed. From these and (17), we see that in the most accurately measured direction, the parameter error was reduced to 2.3% of its initial value, while in the worst direction it remained at 82.4% of the initial value.

As an aside we note that the step size $|\Delta q|$ for the first five iterative steps are 2.5, 9.0e-1, 1.1e-2, 8.7e-5, and 1.6e-6, which shows a linear rate of convergence, as expected.

C. Model 3: Joint Sensor Errors

Instead of lumped errors at the wrist points, an alternative model is to attribute a measurement error to each joint sensor. That is, use (22) as in Model 1. The model equations are

$$f_i = \left\{ \begin{array}{c} [r_1(\theta_i) - r_2(\theta_i)]^2 - d^2 \\ [r_2(\theta_i) - r_3(\theta_i)]^2 - d^2 \\ [r_3(\theta_i) - r_1(\theta_i)]^2 - d^2 \end{array} \right\} = 0,$$
$$i = 1, \cdots, N, \tag{24}$$

where errors enter via θ_i and (18), (22). Accordingly, in the notation of Section II, we have $\bar{x}_i = \bar{\alpha}_i$, $\hat{x}_i = \hat{\alpha}_i$, and $\bar{p}$, $\hat{p}$ as before.

We proceed to analyze the same $N = 12$ measurement samples as in the preceding section. After assigning a variance to the sensor measurement error, we use the same parameter variances as in Section III-A and compute the maximum-likelihood parameter corrections. Using the same standard deviation of 2.5 bits that balanced the chi-square in Model 1, we now get a chi-square of 19.3 compared to an expected value of 36. The detailed results are listed in Tables I and II. The covariance estimates are very similar to those of Model 2, predicting final parameter errors to be 2.5% and 78.0% of the initial value for the best and worst directions, respectively. The sizes of the iterative steps are also similar to those of Model 2, namely, 2.6, 9.1e-1, 1.5e-2, 3.6e-4, and 1.2e-5.

D. Comparison

Two kinds of comparison between the calibrations with and without fixturing are of interest. First, we would like to know if the results are consistent with each other. That is, do the two approaches yield the same parameter values to within the predicted accuracy? Second, we are interested in the relative accuracy of the two calibrations.

From Table I we see that the calibration is robust in the sense that the various models all produce substantially the same parameter corrections. For instance, the difference between the estimates from Models 1 and 2 (Table I) is generally less than the standard deviation reported for Model 2 in Table II and, in the worst case, only 2.3 times the standard deviation. The comparison between Models 1 and 3 is similar. To be more exact, we may compare the results using the covariance formulas found in Appendix III. In particular, "Scenario 1" is of interest because the results of Model 1 come from a separate set of measurements than those reported for Models 2 and 3. The quantity $(p_1 - p_2)^T [\mathrm{Var}\,(p_1 - p_2)]^{-1}(p_1 - p_2)$ should be a chi-square with 18 degrees of freedom. Comparing Models 1 and 2 gives $\chi^2 = 32$, which is at the upper limit of plausibility (probability of being 32 or larger is about 2%). Comparing Models 1 and 3 give $\chi^2 = 27$, which one would expect to exceed about 5% of the time.

Although the final values are not reported in Table I, Model 3 was also run on the fixtured data set. In this case, it is using a subset of the measurements used by Model 1, so we apply the
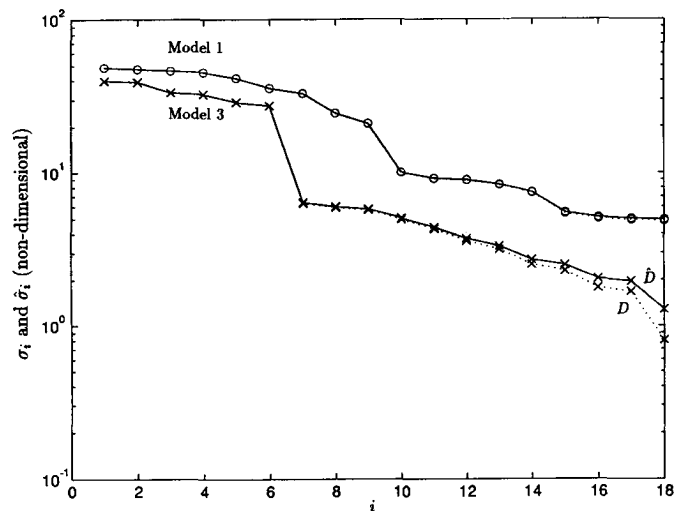

Fig. 2. Singular values for Models 1 and 3.

covariance formula from Scenario 2 of Appendix III. (Model 2 can also compute a calibration on this data set, but the results cannot be directly compared using the same formulas because of the different models of measurement error between Models 1 and 2.) This time we get a chi-square of 11, which is on the low side of 18. However, more than 5% of random samples would be so small, so it is not unreasonable. All in all, Model 3 gives results that are consistent with the results of Model 1. The difference in the two chi-square values (27 versus 11) may indicate that there was some drift in the parameter values between the two experiments. Such a drift was the original motivation for developing a fixtureless calibration method: one can easily recalibrate whenever too much sensor drift has accumulated. However, the difference could also be simply due to chance or possibly due to figments of the modeling and analysis (especially since different covariance formulas apply in the two cases).

The relative accuracies of the calibrations can be judged from Table II. We see that Models 2 and 3 predict virtually the same accuracy, while Model 1 is 1.5 to 6 times more accurate (it varies for different parameters). A different view is presented in Fig. 2 where the singular values s_i of D and $\hat{s}_i = \sqrt{1 + s_i^2}$ of $\hat{D}$ are plotted for Models 1 and 3. Even the most weakly measured directions of parameter error for Model 1 are significantly more accurate than the initial error, so that s_i and $\hat{s}_i$ are virtually identical. This is not true for Model 3, where in the weakest direction the initial error is improved only slightly. We also see that the first 6 singular values for the two experiments are very close, but Model 1 is significantly more accurate thereafter. Of course, due to the fixture, Model 1 collects the equivalent of 9 measurements at each pose versus only 3 for Model 3. However, without the need for a fixture, more poses could easily be sampled to increase the accuracy of Model 3.

It is of interest to note that the slow convergence rate for Model 1 as compared to Models 2 and 3 is related to the pose set used with the fixture. When Model 2 or 3 is applied to the fixtured pose set, a slower rate of convergence also ensues. This correlates with the fact that the condition number
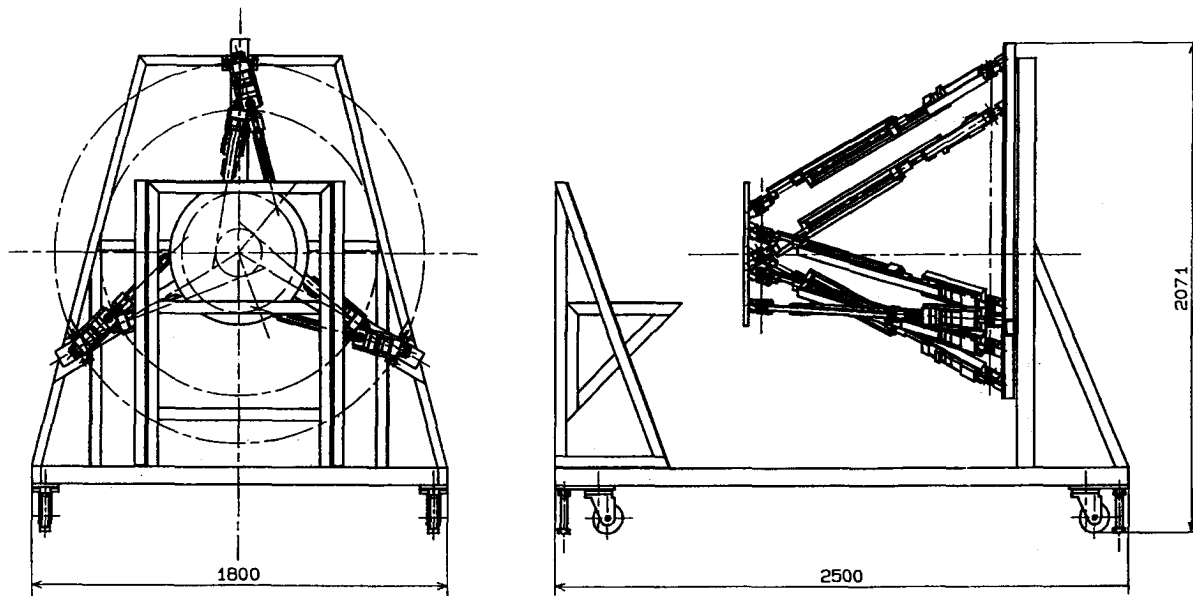
Fig. 3. MEL in-parallel manipulator.

of D for these models is higher for the fixtured pose set than the fixtureless set. The fixtureless set of poses was selected to increase the zone of convergence for the approach of [8]. Here, it has the effect of both speeding up the convergence and making the calibration more accurate.

IV. CALIBRATION OF THE MEL IN-PARALLEL ROBOT

One of the attractive features of in-parallel robot structures is the potential for higher accuracy as compared to serial-link designs, primarily due to the higher stiffness of a closed-loop structure compared to a cantilever. However, this stiffness does not translate directly into better accuracy, rather it implies high repeatability. For example, simulation studies indicate that the manufacturing tolerances one might expect from constructing the relatively large base of an in-parallel robot can lead to significant inaccuracy [19]. Good calibration of the kinematic model is necessary to account for such errors.

The MEL Modified Stewart Platform is shown schematically in Fig. 3. Planar base and end-effector links are connected by 6 legs acting in parallel. Each leg is type RRPRRR, where each prismatic joint is actively controlled via an electric motor and ballscrew, and the rotational joints are passive. Nominally, the first two joints intersect to form a universal joint, and the last three intersect to form a spherical joint. The placement of the joints is unconventional, with the aim of improving the dexterity of the device [20].

The rotational joints on one leg are instrumented using potentiometers and 12-bit A/D converters, providing measurements of the end-effector location via the forward kinematics of the serial linkage formed by the leg. This leg was originally instrumented as a simple solution to the forward kinematics problem, which, if only the leg lengths are measured, is difficult to solve and has multiple solutions. In comparison, the forward kinematics of the single leg is simple when its joint angles are known. After computing an end-effector location using this "measuring leg," the result can be used as the initial

TABLE III
NOMINAL LOCATIONS OF LEG ENDPOINTS FOR MEL ROBOT. ORIGINS ARE AT THE CENTERS OF THE BASE AND ENDPLATE CIRCLES SHOWN IN FIG. 3. ANGLES ARE MEASURED FROM THE RESPECTIVE X-AXES CONSISTENT WITH (25)

Base	B_1	B_2	B_3	B_4	B_5	B_6
radius (mm)	800	600	800	600	800	600
angle (deg)	−90	−90	30	30	150	150
End	E_1	E_2	E_3	E_4	E_5	E_6
radius (mm)	250	100	250	100	250	100
angle (deg)	0	180	120	−60	−120	60

guess to a more exact iterative solution that matches the end-effector location to the remaining leg-length measurements.

The measuring leg can also be used to calibrate the robot. However, we must consider the accuracy of the joint measurements in appraising the accuracy of the calibration result. Moreover, in the case that the measurements yield less accuracy than the original "blueprint" parameter value, we wish to retain the original value. We have seen that the formulation of this paper accommodates this concern.

The nominal kinematics are as follows. The joint axes at the universal and the spherical joint of each leg i ($i = 1, \cdots, 6$) are assumed to intersect in points B_i in the base plate and points E_i in the endplate, respectively. The leg lengths $\ell_i = \|E_i - B_i\|$ are measured using encoders on the drive motors. The base and endplate are both planar, with endpoints given in polar coordinates in Table III. Leg 1 is the measuring leg, having joint rotations of θ_1, θ_2 at the universal joint at the base, leg extension of ℓ_1, and rotation angles of θ_3, θ_4, θ_5 at the spherical joint. In addition, we allow for misalignments in the directions of the joint axes due to manufacturing and assembly errors by including "twist" angles $\beta_1, \cdots, \beta_8$, all nominally zero. (These are the same as Denavit–Hartenburg twist angles, except β_4, β_5 which correspond to Hayati parameters [3], [21], since the joint axes for ℓ_1 and θ_3 are nominally parallel.) Let R_x, R_y, R_z be rotations around the x, y, z axes, respectively, and let T_z be a translation along the z-axis, all of which

we may think of as being standard 4×4 homogeneous tranformation matrices. Accordingly, the kinematic model of the measuring leg can be described succinctly by the sequence of rotations and translations from base to endplate as

$$A(\theta, \beta, \ell_1) =$$
$$R_z(\beta_1)R_x(\theta_1)R_z(\beta_2)R_y(\theta_2)R_x(\beta_3)T_z(\ell_1)R_x(\beta_4)R_y(\beta_5)$$
$$\cdot R_z(\theta_3)R_x(\beta_6)R_y(\theta_4)R_z(\beta_7)R_x(\theta_5)R_z(\beta_8). \qquad (25)$$

As a point of reference for checking, we note that the home position of the robot is defined to be

$$(\ell_1, \cdots, \ell_6) =$$
$$(1423.0, 1301.0, 1423.0, 1301.0, 1423.0, 1301.0)$$

for which the corresponding angles are

$$(\theta_1, \cdots, \theta_5) =$$
$$(-0.6708, -0.1766, 3.1416, -0.1776, -0.6078).$$

All lengths are measured in millimeters (mm) and angles in radian. In the home position (Fig. 3), the endplate is parallel to the base plate and located 1150 mm from it.

A. Initial Error Estimates

To use the maximum-likelihood formulation, we need some initial estimates of the variances of the measurements and the parameter values. To get a rough idea of the variances of the measurements, we performed some preliminary experiments using a digital micrometer. First, we measured joint angle θ_1 using the potentiometer permanently mounted on the robot and at the same time took readings with the micrometer of the displacement of a planar surface on the side of the measuring leg. The leg was rotated through a range of 0.5 rad and we took 3 readings at each of 22 positions. After compensating for a slight geometric nonlinearity to convert the micrometer readings into equivalent angles, we used a least-squares fit to estimate the gain and offset of the potentiometer measurements. This gave a gain of 7.42e-4 rad/bit for the sensor with a residual error having standard deviation of 7.1e-4 rad. That is, the standard deviation of the error is on the order of 1 bit. Also, the measured gain is close to the nominal gain of 7.39e-4 rad/bit, and this gives us a rough idea of the amount of error to expect in sensor gains. Unfortunately, only the first angle could be tested in this fashion, but since all joints use the same sensor hardware, we will assume they all have the same variance. Note that angular errors of 7e-4 rad when multiplied by leg lengths on the order of 1100 mm to 1600 mm yield positional errors on the order of 1 mm.

A potential source of variance in the leg length readings is backlash in the universal and spherical joints. To check this, a second experiment used the micrometer to measure displacements of the endplate as various transient disturbing forces were applied. After the force was removed and vibrations stopped, the displacement consistently settled to within 0.03 mm of the initial position. This implies that the backlash is negligible compared to the error expected from the joint angle sensors.

Finally, we noted that thermal drift in the joint sensors was significant (as much as 5 bits over several hours). By collecting a full set of samples within a 10 minute interval, the drift is made negligible.

B. Modeling

At each sample pose, we measure the joint angles $(\theta_1, \cdots, \theta_5)$ and the leg lengths $(\ell_1, \cdots, \ell_6)$. The kinematics of the device give 5 loop equations at each of N sample poses as follows

$$f_i = \{\ell_j^2 - ||B_1 - B_j + A(\theta, \beta, \ell_1)(E_j - E_1)||^2 = 0,$$
$$j = 2, 3, 4, 5, 6\}, \quad i = 1, \cdots, N, \qquad (26)$$

where the transformation matrix $A(\theta, \beta, \ell_1)$ is as given in (25). Moreover, we do not measure $(\theta_1, \cdots, \theta_5)$ directly, but rather, we obtain A/D readings $(\alpha_1, \cdots, \alpha_5)$ which must be converted to angles by applying the correct gains and offsets, that is,

$$\theta_i = \kappa_i \alpha_i + \theta_i^{\text{off}}, \qquad i = 1, \cdots, 5. \qquad (27)$$

Using the notation of Section II, we have measurements $\overline{x} = (\alpha_1, \cdots, \alpha_5, \ell_1, \ldots, \ell_6)$. As in the case of the RSI Hand Controller experiment, we will calibrate all the legs simultaneously to maximize accuracy. We may arbitrarily pick B_1 and E_1 as the origin points for the base and end plate coordinate systems. Then we have the set of parameters

$$\overline{p} = (B_2, \cdots, B_6, E_2, \cdots, E_6, \beta_1, \cdots, \beta_8,$$
$$\kappa_1, \cdots, \kappa_5, \theta_1^{\text{off}}, \cdots, \theta_5^{\text{off}}, \ell_1^{\text{off}}, \cdots, \ell_6^{\text{off}}).$$

These have corresponding errors $\hat{x}$ and $\hat{p}$. The joint positions $B_2, \cdots, E_6$ have three components each. Thus, there are 54 parameter errors to be estimated.

Not all of the parameters are independently observable. The initial twist β_1 and angle offset θ_1^{off} are indistinguishable from certain displacements of $B_2, \cdots, B_6$ corresponding to rigid-body rotations of the base. A similar confounding exists between angles β_8 and θ_5^{off} and certain rigid-body rotations of $E_2, \cdots, E_6$. Consequently, the parameter set could be reduced by 4, but this requires some care. For example, the angles $\beta_1, \theta_1^{\text{off}}$ could be dropped from the parameter set, but then the *a priori* variances given for errors in the locations of the base points would have to include the proper correlation to account for the rotational errors. It is simpler to keep all of the parameters and let the numerical method separate the dependent and independent errors. We have altogether 54 parameters, of which 50 are independently observable.

The base point errors are not independent. The base plate is constructed of a set of steel U-beams welded together. The base points are mounted in pairs along three beams which radiate from a central hub. A small angular error in the orientation of one of these beams results in a relatively large error common to both base points it carries. Superimposed on this are the independent errors in placing the base pivots onto the beam. We assumed the large common error to have standard deviation of 4 mm and superimposed independent errors of 1 mm. Since B_1 is zero by definition, its neighbor,

B_2, is subject only to the 1 mm deviation. Denoting the 3×3 identity matrix as I_3, we have the following variances and covariances:

$$\text{var}(\hat{B}_2) = I_3,$$
$$\text{var}(\hat{B}_i) = 17I_3, \quad (i = 3, 4, 5, 6)$$
$$\text{cov}(\hat{B}_3, \hat{B}_4) = \text{cov}(\hat{B}_5, \hat{B}_6) = 16I_3.$$

The remaining parameter errors were all assumed to be independent. The standard deviations were as follows: 3 mm for each component of $E_2, \cdots, E_6$, 100 bits for the angle offset, 10 mm for leg length offset, 0.08 radian for twist angles, 10% for the sensor gain.

For the sensor errors, we assumed 2 bits for the angle measurements and 0.03 mm for the leg lengths. The latter is so small that it can be neglected with virtually no change in the results.

C. Pose Selection and Sampling Procedure

At each pose, there are 11 measurements, which is an excess of five beyond the six degrees of freedom of the device. Consequently, 20 poses provide a total of 100 excess measurements from which we will extract the 50 independent parameters. Such a twice-over sampling is a minimally acceptable level of oversampling, which we thought would be sufficient for our investigative study.

Of the 20 poses, we chose the first 13 to lie near the limit of one or more of the leg lengths, each of which may vary from 1.18 m to 1.6 m. These poses fall near the positional boundaries of the workspace. The last 7 lie near the center of the workspace, with angular displacements near the limits allowed by link collisions. The poses were not optimized with respect to the conditioning of the fitting matrix, although this would most likely have improved the result.

The robot was moved to each successive pose under computer control. To be sure that the robot was at rest, the samples were not recorded until the leg readings from two samples taken 1 s apart agreed to full precision. Due to integral control, the leg readings consistently settled to within 0.001 mm of the commanded values. By taking samples at steady state, we avoid errors of dynamic deflection of the robot structure and errors due to asynchronous measurement of the leg lengths and joint angles.

The sampling process takes about 5 min, mostly spent waiting for steady state. Three such samples taken within 25 min agreed with each other to within ± 1 bit. These sample sets were taken by progressing through the poses in exactly the same order. Subsequently we have realized that a random progression would have been preferable, as the effects of backlash would then have been made more apparent.

To remove the bulk of sensor drift error, an offset was computed for each joint to make the first pose agree exactly with the nominal kinematic model. This pose corresponds to the robot's "home" position.

D. Results and Discussion

Fig. 4 shows the singular values for the fitting matrix D and the augmented fitting matrix $\hat{D}$. We see that the experiment
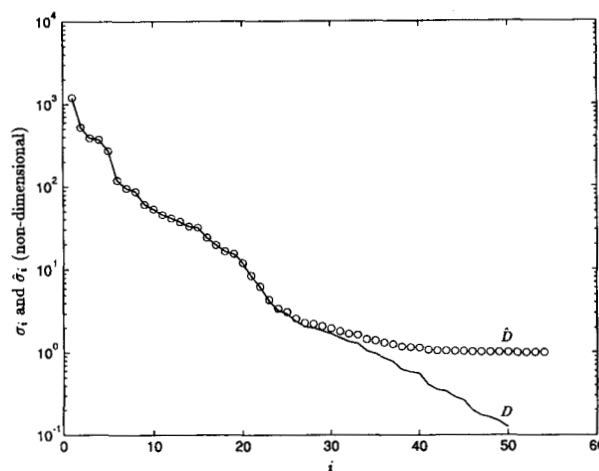

Fig. 4. Singular values for calibration of the MEL in-parallel manipulator.

reduces the first 20 error components to less than 10% of their initial values. After that the effectiveness of the calibration continues to decay, and beyond the 40th error component virtually no information is gained. Singular values $\sigma_{51}, \cdots, \sigma_{54}$ were computed as less than 10^{-13}, which numerically verifies that $4°$ of freedom in the model are unobservable. It is not necessary to reduce the model by removing the poorly identified parameters; this is done automatically by the least-squares weighting of the initial parameter variances. This is seen to happen in the figure where the two sets of singular values separate, and those of $\hat{D}$ approach unity (10^0). The final 4 unobservable parameter combinations will remain exactly at their initial values.

The expected value of χ^2 is 100 with standard deviation 14.1. The experiment gives a value of $\chi^2 = 128.0$, which is about 2 standard deviations from the expected value. We have forced the χ^2 to a reasonable value by inflating the standard deviation of the angle measurements to 2 bits, as opposed to the 1 bit deviation we measured in the preliminary experiment in Section IV-A. In making this adjustment, the variance Σ_q that we compute becomes larger and more accurately reflects the actual accuracy of the experiment.

Of the 54 parameters, only 36 have an effect on the accuracy of the calibrated robot: these are the 30 coordinates of the pivot points and the 6 leg length offsets. The other 18 are all parameters of the measuring leg (potentiometer gains and offsets, joint twists), which we need for the calibration but do not use for robot control. The covariance matrix for the final parameter errors Σ_p' (16) is a symmetric 54×54 matrix containing the complete picture of the accuracy of the experiment. However, to briefly summarize the results, we may compare the entries of $(\Sigma_p')^{1/2}$ with the initial $\Sigma_p^{1/2}$, particularly directing our attention to the diagonal entries. By this measure, we see that the base pivot uncertainties have been reduced from 3.4 mm to approximately 2.3–2.9 mm, the endplate pivots from 3 mm to 1.3–2 mm and the leg length offsets from 10 mm to about 4 mm. The uncertainty in the pivot locations is commensurate with the sensor accuracy, because a 2 bit sensor error translates into about 2 mm of positional error. As for the measuring leg, potentiometer

offsets were reduced from 100 bits to 8–27 bits, potentiometer gains from 10% uncertainty to 0.2%, and twist angles from 0.08 rad to 0.002 rad.

It may be instructive to note that in our first attempts at computing a calibration, the parameter set was smaller: it had only 50 parameters, all observable. This was accomplished by constraining the coordinates of certain base and endplate pivots. Also, the base pivot variances were all assumed independent with standard deviation 3 mm. These seemingly innocuous differences had a profound effect: the angle error had to be inflated to 5 bits to bring χ^2 down to 124. Otherwise the variance of the base pivots would have needed to be implausibly large (>10 mm). So the chi-square check indicated definitively that the initial model was insufficient.

Even now, the necessity of inflating the angle errors to 2 bits indicates that there may be some missing unmodeled effect. For example, twist angles $R_y(\beta_0)$ and $R_y(\beta_9)$ pre- and post-multiplying $A(\theta, \beta, \ell_1)$ could be considered. There are many more kinematic parameters that are possible if we consider that the axes in the spherical joints may not truly intersect. Some other possible factors are backlash, elastic deformation due to gravity, or eccentricities in the mounting of the potentiometers.

The greatest improvement in the calibration would not come from explaining the source of this last bit of error. Instead it would come from fundamental improvements in the experiment itself. The most important action would be to improve the joint angle sensors. We made use of potentiometers that had been installed for a different purpose requiring less accuracy. Another important action would be to improve the pose selection and perhaps include more poses. After these have been done, one could determine with greater confidence whether or not a significant unmodeled factor is present. It may then become the limiting factor in the accuracy of the calibration.

V. SUMMARY AND CONCLUSION

We have presented a method of analysis for calibrating mechanisms having closed kinematic chains. It applies equally well to open-chain mechanisms with endpoint sensing. Measurement errors and kinematic errors (such as backlash) may enter the kinematic equations in implicit form, hence we call the formulation an "implicit loop method." The methodology has been demonstrated in experiments on two different devices, thus illustrating the generality of the approach and exploring its behavior on real examples. Features of the method include:

- initial variance estimates provide rational scaling factors for distributing errors between multiple sources,
- "input" and "output" errors are treated in a uniform manner,
- the use of prior estimates on the parameters damps out poorly calibrated parameters or combinations of parameters, hence the inclusion of an insignificant parameter has little or no effect on the final result,
- the method calculates the variance of the parameter estimates,
- and a chi-square calculation tests the goodness of fit of the model, helping to detect unmodeled factors.

The method is based on the maximum-likelihood principle that results in a nonlinear least-squares problem to be solved. We outline an iterative numerical scheme, which displays a linear rate of convergence on the experimental problems.

To illustrate the method, we re-analyze the experimental data of [8] for the RSI Hand Controller. The flexibility of the approach is demonstrated by performing the calibration using two different models of the error: one lumps the errors at the wrist points in the manner of [8], whereas the other attributes the errors to the joint measurements. A calibration using only the joint angle measurements was found to be consistent, although less accurate, than a calibration for the same experiment using additional pose information from a fixturing device. The difference is attributable to the 6 extra measurements per pose provided by the fixture. The results for a second set of experimental data (not using the fixture poses) are also consistent with the fixtured result, although a chi-square test shows a larger discrepancy in this case. This may be due to a slight drift in the potentiometers between the experiments: the motivation for the calibration was to compensate for this kind of drift.

The MEL in-parallel robot has also been calibrated by this method. Although the resolution of the sensors was found to be insufficient to perform a highly accurate calibration, the applicability of the method is demonstrated. Our initial model was shown to be insufficient to meet the goodness of fit criterion. The explanation was found to be related to small angular errors in mounting the measuring leg on the base frame. These errors are not independently observable from certain rigid-body displacements of the base frame. This could have been addressed without increasing the parameter set by introducing the appropriate correlated uncertainty in the pivot locations, but since the formulation is impervious to overparameterization, it was much simpler to directly add the angular parameters to the model. This illustrates one of the primary features of the approach.

The work on the MEL arm neglected the important issue of pose selection. However, for the RSI Hand Controller, Hollerbach and Lokhurst [8] addressed pose selection as a means of improving the convergence zone of their closed-loop calibration. We find that the poses they selected on this basis also increase the smallest singular value of the fitting matrix, which has the effect of decreasing the error in the calibrated parameters. Pose selection criteria and algorithms as discussed in [22]–[24] require only minor modifications to be applied for the implicit loop formulation. Whatever approach is used in this regard, once a set of poses has been chosen and a set of measurements has been taken, the methods described herein form a good methodology for computing the calibrated parameters and testing the validity of the model.

As a final caveat, we note that a goodness-of-fit calculation checks the consistency between experiment and mathematical model. As such, a bad fit clearly indicates a problem, but a good fit does not guarantee success. If the experiment includes direct measurement of the end-effector, the residuals on those measurements give a strong test of success. If there are no such measurements, as can be the case with closed-loop linkages,

independent experiments may be advisable to verify the final accuracy.

APPENDIXES: DERIVATIONS

I. ITERATIVE METHOD

Following the notation of Section II, collect all of the normalized measurement errors y_i into one $Nk \times 1$ column $y = (y_1^T \cdots y_N^T)^T$. Similarly, collect all the residuals $f(x_i, p)$ into one $Nm \times 1$ column F. Then we may rewrite the minimization problem of (7)–(8) as: find Δy and Δq to minimize

$$(y + \Delta y)^T (y + \Delta y) + (q + \Delta q)^T (q + \Delta q) \qquad (A.1)$$

subject to the linearized constraints

$$J_y \Delta y + J_q \Delta q = -F, \qquad (A.2)$$

where the Jacobian matrices have block entries in accordance with (8). Using the QR-decomposition $QR = J_y^T$, we may pre-multiply both sides of (A.2) by the nonsingular matrix R^{-T} to get

$$Q^T \Delta y + D \Delta q = -R^{-T} F, \qquad (A.3)$$

where $D = R^{-T} J_q$. Matrix Q is an $Nk \times Nm$ matrix $(k \geq m)$ having orthogonal columns. We can complete the basis with an $Nk \times N(k - m)$ matrix Q' such that $(Q \quad Q')$ is orthogonal. Then the minimization criterion (A.1) may be written as

$$\|Q^T (y + \Delta y)\|^2 + \|Q'^T (y + \Delta y)\|^2 + \|q + \Delta q\|^2. \quad (A.4)$$

Since $Q'^T (y + \Delta y)$ does not appear in the constraint, the minimum will have

$$Q'^T (y + \Delta y) = 0. \qquad (A.5)$$

Re-arranging (A.3) and adding $Q^T y$ to both sides, we have

$$Q^T (y + \Delta y) = Q^T y - D \Delta q - R^{-T} F. \qquad (A.6)$$

Substitute (A.5)–(A.6) into (A.4) to express the minimization criterion as

$$\|Q^T y - D \Delta q - R^{-T} F\|^2 + \|q + \Delta q\|^2. \qquad (A.7)$$

This is now an unconstrained minimization involving only Δq. Its solution is the same as the least-squares solution of the linear system

$$\begin{pmatrix} D \\ I \end{pmatrix} \Delta q = \begin{pmatrix} Q^T y - R^{-T} F \\ -q \end{pmatrix}. \qquad (A.8)$$

Combining (A.5)–(A.6) into one matrix equation and pre-multiplying by $(Q \quad Q')$, one obtains

$$y + \Delta y = Q(Q^T y - D \Delta q - R^{-T} F). \qquad (A.9)$$

After sorting out the block form of the equations, one sees that (A.8)–(A.9) are identical to (12)–(13) of Section II-B.

II. APPROXIMATE COVARIANCE OF THE ESTIMATE

Recall that the mean of an $n \times 1$ vector of random variables x is denoted $E(x)$ (expected value). The covariance of x is an $n \times n$ matrix $\text{Var}(x) = E\{[x - E(x)][x - E(x)]^T\}$. If A is a constant matrix, then $E(Ax) = AE(x)$ and $\text{Var}(Ax) = A\text{Var}(x)A^T$.

Let us assume that the estimate $z = (y, q)$ and the true value $z^* = (y^*, q^*)$ are sufficiently small so that the linearization of the kinematic equations F about the initial guess $(y, q) = 0$ is accurate. Then, denoting the Jacobian matrix $J = (J_y \quad J_q)$, we have the linearization

$$F(z^*) = F(0) + Jz^*.$$

But the kinematic equations must be satisfied at the true values, i.e., $F(z^*) = 0$, so

$$F(0) = -Jz^*. \qquad (A.10)$$

From (A.1)–(A.2), the first step of the iterative procedure gives

$$z = -J^+ F(0), \qquad (A.11)$$

which is the final estimate when F is linear. Together these give the error in the estimate as

$$z - z^* = (J^+ J - I)z^*. \qquad (A.12)$$

From this we have that the estimation error has zero mean:

$$E(z - z^*) = (J^+ J - I)E(z^*) = 0, \qquad (A.13)$$

that is, the estimated is unbiased.

We want to isolate the covariance matrix of the error in the estimates of the parameters $q = (0 \quad I)z$, which can be written using (A.12) as

$$\text{Var}(q - q^*) = (0 \quad I)(J^+ J - I)$$
$$\cdot \text{Var}(z^*)(J^+ J - I)^T \begin{pmatrix} 0 \\ I \end{pmatrix}. \quad (A.14)$$

But z^* are normalized error variables (see Section II-B), so $\text{Var}(z^*) = I$. For any nonsingular matrix A, we have the identity $J^+ J = (AJ)^+(AJ)$, and in particular, if J_y is nonsingular, this is true for $A = R^{-T}$. So we may replace J in (A.14) with $R^{-T} J = (Q^T \quad D)$. Using these facts and the relations $J^+ = J^T (JJ^T)^{-1}$ and $Q^T Q = I$, we write

$$(0 \quad I)(J^+ J - I) = D^T (I + DD^T)^{-1}(Q^T \quad D) - (0 \quad I). \qquad (A.15)$$

Using the identity $D^T (I + DD^T)^{-1} = (D^T D + I)^{-1} D^T$, (A.15) becomes

$$(0 \quad I)(J^+ J - I) = (D^T D + I)^{-1}(D^T Q^T \quad -I). \quad (A.16)$$

Substituting this expression twice into (A.14), we obtain

$$\text{Var}(q - q^*) = (D^T D + I)^{-1}(D^T D + I)(D^T D + I)^{-1}$$
$$= (D^T D + I)^{-1}. \qquad (A.17)$$

By the definition of the augmented fitting matrix $\hat{D}$ [Section II-C, (14)] this is

$$\text{Var}(q - q^*) = (\hat{D}^T \hat{D})^{-1}, \qquad (A.18)$$

which justifies (15) of Section II-C.

III. COMPARING EXPERIMENTS

We want to establish chi-square criteria for judging whether two calibration experiments on the same device have obtained the same result to within the predicted covariance of the estimation procedure. Let the measurement errors for the two experiments be y_1^* and y_2^* so that the complete set of measurement and parameter errors is $z^* = (y_1^*, y_2^*, q^*)$. By (A.12), there are matrices A_1 and A_2 such that the estimation errors are of the form

$$q_1 - q^* = A_1 z^*, \qquad q_2 - q^* = A_2 z^*.$$

Accordingly, the difference in the estimates has expected value of zero:

$$E(q_1 - q_2) = E[(q_1 - q^*) - (q_2 - q^*)]$$
$$= (A_1 - A_2)E(z^*) = 0.$$

The covariance matrix for the difference is

$$\text{Var}(q_1 - q_2) = \text{Var}[(A_1 - A_2)z^*]$$
$$= (A_1 - A_2)(A_1 - A_2)^T.$$

Since $\text{Var}(q_1 - q^*) = A_1 A_1^T$ and $\text{Var}(q_2 - q^*) = A_2 A_2^T$, we have

$$\text{Var}(q_1 - q_2) = \text{Var}(q_1 - q^*) + \text{Var}(q_2 - q^*)$$
$$- A_1 A_2^T - A_2 A_1^T. \qquad (A.19)$$

To test the agreement between the experiments, we may compute

$$(q_1 - q_2)^T [\text{Var}(q_1 - q_2)]^{-1} (q_1 - q_2),$$

which will be a chi-square with n degrees of freedom. Now we want to specialize this to two scenarios.

Scenario 1: Two independent sets of measurements are used to obtain parameter estimates q_1 and q_2, each starting from the same *a priori* information. Following the notation of Appendix II, we write

$$A_1 = (D_1^T D_1 + I)^{-1}(D_1^T Q_1^T \quad 0 \quad -I)$$
$$A_2 = (D_2^T D_2 + I)^{-1}(0 \quad D_2^T Q_2^T \quad -I). \qquad (A.20)$$

Accordingly,

$$A_1 A_2^T = (D_1^T D_1 + I)^{-1}(D_2^T D_2 + I)^{-1}$$
$$= \text{Var}(q_1 - q^*)\text{Var}(q_2 - q^*). \qquad (A.21)$$

Substituting this and its transpose into (A.19), one obtains

$$\text{Var}(q_1 - q_2) = \text{Var}(q_1 - q^*) + \text{Var}(q_2 - q^*)$$
$$- \text{Var}(q_1 - q^*)\text{Var}(q_2 - q^*)$$
$$- \text{Var}(q_2 - q^*)\text{Var}(q_1 - q^*). \qquad (A.22)$$

Scenario 2: Parameter estimate q_1 is found using a subset of the measurements used for estimate q_2, each time starting from the same *a priori* information. In this case, we have

$$A_1 = (D_1^T D_1 + I)^{-1}(D_1^T Q_1^T \quad 0 \quad -I)$$
$$A_2 = (D_1^T D_1 + D_2^T D_2 + I)^{-1}(D_1^T Q_1^T \quad D_2^T Q_2^T \quad -I)$$

from which one obtains

$$A_1 A_2^T = (D_1^T D_1 + I)^{-1}(D_1^T D_1 + I)(D_1^T D_1 + D_2^T D_2 + I)^{-1}$$
$$= (D_1^T D_1 + D_2^T D_2 + I)^{-1}$$
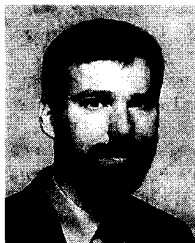$$= \text{Var}(q_2 - q^*). \qquad (A.23)$$

Substituting this and its transpose into (A.19), one obtains

$$\text{Var}(q_1 - q_2) = \text{Var}(q_1 - q^*) - \text{Var}(q_2 - q^*). \qquad (A.24)$$

REFERENCES

[1] J. M. Hollerbach and C. W. Wampler, "A taxonomy for robot kinematic calibration methods," *Int. J. Robotics Res.*, to be published.
[2] Z. S. Roth, B. W. Mooring, and B. Ravani, "An overview of robot calibration," *IEEE Trans. Robot. Automat.*, vol. RA-3, no. 5, pp. 377–385, 1987.
[3] J. M. Hollerbach, "A survey of kinematic calibration," in *The Robotics Review 1*, O. Khatib, J. Craig, and T. Lozano-Perez, Eds. Cambridge, MA: MIT Press, 1989, pp. 207–242.
[4] B. Karan and M. Vukobratović, "Calibration and accuracy of manipulation robot models—An overview," *Mech. Mach. Theory*, vol. 29, no. 3, pp. 479–500, 1994.
[5] L. J. Everett and C. Y. Lin, "Kinematic calibration of manipulators with closed loop actuated joints," in *Proc. IEEE Int. Conf. Robotics Automat.*, Philadelphia, PA, Apr. 24–29, 1988, vol. 2, pp. 792–797.
[6] H. Zhuang and Z. S. Roth, "A method for kinematic calibration of Stewart platforms," in *Proc. ASME Winter Annu. Meet.*, Atlanta, GA, Dec. 1–6, 1991, ASME DSC-vol. 29, pp. 43–48.
[7] D. J. Bennett and J. M. Hollerbach, "Autonomous calibration of single-loop closed kinematic chains formed by manipulators with passive endpoint constraints," *IEEE Trans. Robot. Automat.*, vol. 7, no. 5, pp. 597–606, 1991.
[8] J. M. Hollerbach and D. M. Lokhurst, "Closed-loop kinematic calibration of the RSI 6-DOF hand controller," *IEEE Trans. Robot. Automat.*, 1995, to be published. Preliminary version available in
[9] *Proc. IEEE Int. Conf. Robot. Automat.*, Atlanta, GA, May 2–7, 1993, vol. 2, pp. 142–148.
[10] A. Nahvi, J. M. Hollerbach, and V. Hayward, "Calibration of a parallel robot using multiple kinematic closed loops," in *Proc. IEEE Int. Conf. Robot. Automat.*, San Diego, CA, May 8–13, 1994, vol. 1, pp. 407–412.
[11] C. Wampler and T. Arai, "Calibration of robots having kinematic closed loops using nonlinear least-squares estimation," in *Proc. IFToMM-jc Symp.*, Nagoya, Japan, Sept. 24–26, 1992, vol. 1, pp. 153–158.
[12] J.-M. Renders, E. Rossignol, M. Becquet, and R. Hanus, "Kinematic calibration and geometrical parameter identification for robots," *IEEE Trans. Robot. Automat.*, vol. 7, no. 6, pp. 721–732, 1991.
[13] G. Zak, B. Benhabib, R. G. Fenton, and I. Saban, "Application of the weighted least squares parameter estimation method to the robot calibration," *Trans. ASME, J. Mech. Design*, vol. 116, no. 3, pp. 890–893, 1994.
[14] A. V. Huffel and J. Vandewalle, *The Total Least Squares Problem: Computational Aspects and Analysis*. Philadelphia, PA: SIAM, 1991.
[15] H. Schwetlick and V. Tiller, "Numerical methods for estimating parameters in nonlinear models with errors in the variables," *Technometrics*, vol. 27, no. 1, pp. 17–24.
[16] P. T. Bogss, R. H. Byrd, and R. B. Schnabel, "A stable and efficient algorithm for nonlinear orthogonal distance regression," *SIAM J. Sci Stat. Comput.*, vol. 8, no. 6, pp. 1052–1078, 1987.
[17] A. E. Bryson and Y.-C. Ho, *Applied Optimal Control: Optimization, Estimation, and Control*, Washington, DC: Hemisphere Publ. Corp., 1975.

[18] W. H. Press, B. P. Flannery, S. A. Teukolsky, and W. T. Vetterling, *Numerical Recipes: The Art of Scientific Computing.* Cambridge, UK: Cambridge Univ. Press, 1986.

[19] A. Gelb, Ed., *Applied Optimal Estimation.* Cambridge, MA: MIT Press, 1986.

[20] J. Wang and O. Masory, "The effect of manufacturing tolerances on Stewart platform accuracy," in *Proc. 5th Annu. Conf. Recent Advances in Robotics,* Florida Atlantic Univ., June 11–12, 1992, pp. 165–178.

[21] R. S. Stoughton and T. Arai, "A modified Stewart platform manipulator with improved dexterity," *IEEE Trans. Robotics Automat.,* vol. 9, no. 2, pp. 166–173, 1993.

[22] S. A. Hayati, "Robot arm geometric link parameter estimation," in *Proc. 22nd IEEE Conf. Decision and Control,* San Antonio, TX, Dec. 14–16, 1983, pp. 1477–1483.

[23] H. Zhuang, K. Wang, and Z. S. Roth, "Optimal selection of measurement configurations for robot calibration using simulated annealing," in *Proc. IEEE Conf. Robot. Automat.,* San Diego, CA, May 8–13, 1994, vol. 1, pp. 393–398.

[24] J. H. Borm and C. H. Menq, "Determination of optimal measurement configurations for robot calibration based on observability measure," *Int. J. Robotics Res.,* vol. 10, no. 1, pp. 51–63, 1991.

[25] M. R. Driels and U. S. Pathre, "Significance of observation strategy on the design of robot calibration experiments," *J. Robotic Syst.,* vol. 7, no. 2, pp. 197–223, 1990.

John M. Hollerbach (M'85) received the B.S. degree in chemistry (1968) and the M.S. degree in mathematics (1969) from the University of Michigan, Ann Arbor, and the S.M. (1975) and Ph.D. (1978) degrees from MIT, Cambridge, in computer science.

He is Professor of Computer Science at the University of Utah. From 1989 to 1994 he was the Natural Sciences and Engineering/Canadian Institute for Advanced Research Professor of Robotics at McGill University, jointly in the Departments of Mechanical Engineering and Biomedical Engineering. From 1982 to 1989 he was on the faculty of the Department of Brain and Cognitive Sciences and a member of the Artificial Intelligence Laboratory at MIT; from 1978 to 1982 he was a Research Scientist there. He has published many papers in the area of robotics and biological motor control, has co-authored the book *Model-Based Control of a Robot Manipulator* (MIT Press, 1988), and has co-edited the books *Robot Motion: Planning and Control* (MIT Press, 1982) and *Vision and Action: An Invitation to Cognitive Science, vol. 2* (MIT Press, 1990).

In 1984 Dr. Hollerbach received an NSF Presidential Young Investigator Award; in 1988 he was named a Fellow of the Canadian Institute for Advanced Research. He was the Program Chairman of the 1989 IEEE International Conference on Robotics and Automation, and a member of the Administrative Committee of the IEEE Robotics and Automation Society from 1989 to 1993. He is a Technical Editor of the IEEE TRANSACTIONS ON ROBOTICS AND AUTOMATION, Treasurer of the *IEEE/ASME Journal of Microelectromechanical Systems,* and a Senior Editor of *Presence: Teleoperators and Virtual Environments.*

Charles W. Wampler (M'87) received the B.S. degree (1979) from MIT, and the M.S. (1980) and Ph.D. (1985) degrees from Stanford University, Stanford, CA, all in mechanical engineering.

He is Staff Research Scientist in the Mathematics Department of the General Motors Research and Development Center, Warren, MI. In 1992, he worked in Japan as a Guest Researcher at the Mechanical Engineering Laboratory, Tsukuba. His major research interest has been the kinematics of robots and mechanisms, including kinematically redundant robots, in-parallel manipulators, and the analysis and synthesis of mechanisms. In recent years, he has contributed to the development and application of polynomial continuation, a numerical method for solving systems of polynomial equations.

Dr. Wampler is a member of the American Society of Mechanical Engineers.

Tatsuo Arai (M'87) received the B.S., M.S., and Ph.D. degrees in instrumentation and mathematical engineering from the University of Tokyo in 1975, 1977, and 1986, respectively.

He joined the Mechanical Engineering Laboratory, Tsukuba, Ibaraki, Japan, in 1977 and is currently a Director of the Autonomous Machinery Division. He is also a Lecturer in Mechanical Engineering at the University of Chiba. He spent one year at MIT as a Visiting Scientist working on mechanism analysis and synthesis of parallel manipulators. Since 1977, his major research interests have been robotics, especially, mechanism and motion control for manipulators, teleoperation, parallel manipulators, micro machines, and autonomous systems.

Dr. Arai is a member of the Japan Society of Mechanical Engineers, the Society of Instrumentation and Control Engineers, and the Robotics Society Japan.